Reductive Activation of Tripod Cobalt Compounds: Oxidative Addition of H−H, P−H, and Sn−H Functions

Ute Winterhalter,[a] Laszlo Zsolnai,[a] Peter Kircher,[a] Katja Heinze,[a] and Gottfried Huttner*[a]

Dedicated to Prof. Dr. Peter Paetzold on the occasion of his 65th birthday

Keywords: Tripodal ligands / Cobalt / Reductive activation / Oxidative addition / Tin hydrides / Diphosphene

Treatment of the *tripod* compounds *tripod*$CoCl_2$ (**1**), and *tripod*CoCl (**2**), [*tripod* = $CH_3C(CH_2PPh_2)_3$] in THF solution under argon atmosphere with strong reducing agents such as KC_8 leads to the generation of reactive species. While the dinitrogen compound *tripod*$Co(N_2)$Co*tripod* (**3**), which is formed under N_2 atmosphere, is rather unreactive, the species formed under argon atmosphere undergo selective reactions with compounds containing P–H or Sn–H functions. With $PhPH_2$ as the reagent, the diphosphene compound *tripod*Co(η^2-PhP=PPh) (**8**), is formed in a yield (44%) similar to that achieved in the preparation of **8** from **2** and PhPHNa (60%). With Ph_3SnH as the reagent, *tripod*$CoSnPh_3$ (**9**), is obtained (yield 61%), while reaction with Bu_3SnH produces *tripod*$Co(H)_2SnBu_3$ (**10a**, 50%). The Co^I species **9** undergoes oxidative addition of dihydrogen to produce the Co^{III} compound *tripod*$Co(H)_2SnPh_3$ (**10b**), which is an analogue of **10a**. The properties of these new compounds are characterized by the usual analytical techniques, including NMR spectroscopy, cyclic voltammetry, and X-ray analysis.

Introduction

The chemistry of [*tripod*Co] templates − *tripod* = $CH_3C(CH_2PPh_2)_3$ − is well developed for the Co^{II} [1] and Co^{III} [2] oxidation states, while low-valent derivatives are still rare. On the other hand, it is well-known that templates L_3Co (L = PMe_3)[3] also possess a rich chemistry with Co in lower oxidation states. A possible entry into the chemistry of low-valent [*tripod*Co] compounds is the reduction of easily accessible [*tripod*Co^{II}] compounds such as *tripod*$CoCl_2$ (**1**) (Scheme 1),[4] by electropositive metals. Using zinc powder as the reductant,[5] the Co^I compound *tripod*CoCl (**2**), is produced,[4,6] which in itself allows access to the chemistry of [*tripod*Co^I] derivatives.[5] Reduction of **1** with Na/Hg has been found to produce *tripod*$Co(N_2)$Co*tripod* (**3**).[7]

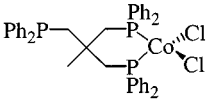

1

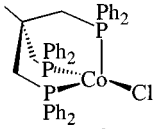

2

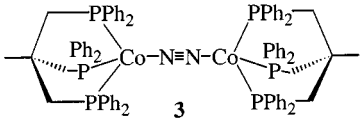

3

Scheme 1

The Co^0 compound **3** has already been tested with regard to its propensity to act as a precursor for other low-valent [*tripod*Co] species.[8] It was found, however, to be rather unreactive, while the solutions from which it is obtained are reactive due to the presence of some undefined by-products.[8] Although the reactions of such solutions with CO_2 or CS_2 furnished only the oxidized products incorporating η^2-CO_3 and η^2-S_2CO ligands,[8] their observed reactivity indicates that reduction of the metal in **1** produces highly reactive species.

In this paper, we report on the results obtained upon reduction of **1** in THF solution by KC_8 or activated Mg (Scheme 2). While *tripod*$Co(N_2)$Co*tripod* (**3**), is obtained as one of the products when this reduction is carried out under dinitrogen, reduction under argon atmosphere produces highly reactive species that undergo oxidative addition with P−H and Sn−H functions, thereby leading to derivatives such as *tripod*$Co(P_2Ph_2)$ (**8**), and *tripod*$Co(H)_2(SnR_3)$ (**10**).

Results and Discussion

Reductions of 1 and 2: Products and By-Products

Products

Reduction of a THF solution of **1** with various reductants was monitored by UV/Vis/NIR spectrophotometry,

[a] Anorganisch-Chemisches Institut der Universität Heidelberg, Im Neuenheimer Feld 270, 69120 Heidelberg, Germany
Fax: (internat.) + 49-(0)6221/545707

  1434−1948/01/0101−0089 $ 17.50+.50/0

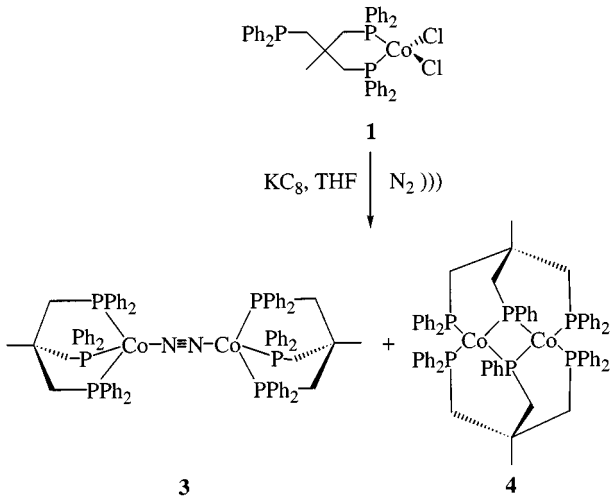

Scheme 2

this being the only simple tool suitable for analysing these highly sensitive and strongly paramagnetic solutions. Reduction with KC_8 as well as with Na/Hg under N_2 was found to produce solutions showing a strong band at around 1130 nm and a weaker absorption at around 680 nm (Figure 1b; Table 1). The relative intensities of these two bands was found to vary to some extent in different experiments, while no conditions could be found under which one of these two bands was absent. Reduction of **1** under an N_2 atmosphere with activated Mg led to spectra of type a (Figure 1a) with just one prominent band at 1130 nm. The same type of spectrum was obtained when **2** was reduced with KC_8 under N_2. Reduction of **1** or **2** under argon atmosphere with KC_8 produced solutions that characteristically showed spectra of type c (Figure 1c). The same type of spectrum was observed when **1** was reduced with Na/Hg under Ar. If the spectrum contained any signature of *tripod*-Co(N_2)Co*tripod*, **3**, this should be the band at around 1130 nm (Figure 1a). For comparison purposes, **3** was prepared by reacting **2** with KC_8 under N_2. On layering the THF solution obtained by this procedure with petroleum ether (boiling range 40−60 °C), crystals of **3** were produced. These crystals were analysed by measuring the lattice constants [a = 1794(3) pm, b = 1531.1(9) pm, c = 1279(1) pm, α = 90°, β = 94.16(6)°, γ = 90°], which were found to be identical to those reported for **3** in the literature.[7] The UV/Vis/NIR spectrum of a solution of this authentic crystalline sample of **3** in THF was recorded. The band at around 1130 nm (Figure 1a) was found to coincide with the intrinsic absorption of **3** [λ_{max} (ε) = 405 (8000), 718 (550), 1134 nm (4700) $M^{-1}cm^{-1}$]. This result, together with the result obtained by comparing the UV/Vis/NIR spectra in Figure 1 (a, b: N_2 atmosphere; c: Ar atmosphere), indicates that the compound giving rise to the band at 1130 nm, which is only present when the experiment is performed under N_2, is the dinitrogen compound **3** itself. The compound giving rise to the band at 680 nm (Figure 1, b and c) is not identified as such. Again, on the basis of the UV/Vis/NIR spectra, it cannot be the Co^I species *tripod*CoCl that shows a completely different spectrum[4] [λ_{max} (ε) = 530 (120, sh), 826 (150), 1131 (430), 1224 (450) $M^{-1}cm^{-1}$].

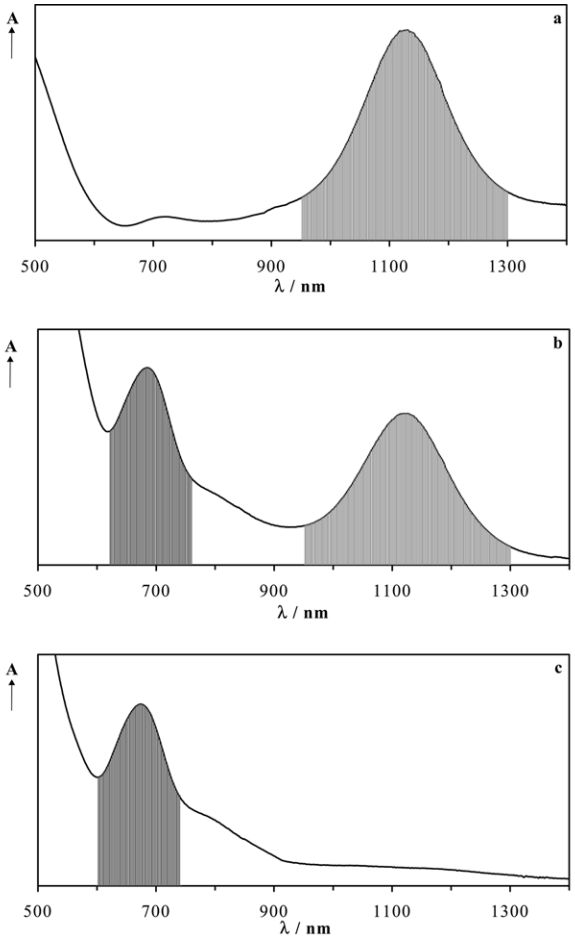

Figure 1. Electronic spectra of solutions obtained by reducing THF solutions of **1** or **2** under N_2 or Ar.
a: Spectrum of **3**, N_2 atmosphere. − **b**: Spectrum observed after reducing **1** or **2** under an N_2 atmosphere; for experimental conditions, see Table 1. − **c**: As **b**, but with Ar atmosphere instead of N_2; for experimental conditions, see Table 1

Table 1. Starting compounds, reductants, and inert gases used to produce compounds with the spectral signature shown in Figure 1

Comp.	Reductant	Atmosphere	Spectrum
1	Mg	N_2	a
2	KC_8	N_2	a
1	KC_8	N_2	b
1	Na/Hg	N_2	b
1	KC_8	Ar	c
2	KC_8	Ar	c
1	Na/Hg	Ar	c

By-Products

The nature of the compound giving rise to the absorption at 680 nm is not known. It is, however, known that this species is the reactive one since **3** (band at 1130 nm, Figure 1a and 1b) is unreactive with respect to the reactions reported in this paper. Only solutions showing the absorption at 680 nm have been found to undergo reactions with

the reagents used. Among the products generated upon reduction of **1**, the dicobalt species $[CH_3C(CH_2PPh_2)_2CH_2PPh]_2Co_2$ (**4**), is occasionally obtained in low yields in the form of a crystalline material.

The constitution of **4** shows that it is only a minor by-product that cannot be responsible for the generation of the compounds obtained upon reactions of solutions showing the band at 680 nm with various substrates (see later). Thus, **4** has been dephenylated at the *tripod* ligand, whereas all the products described herein contain an intact ligand. The FAB mass spectrum of crystalline **4** shows peaks at m/z = 1212 [M^+] and 606 [M^{2+}]. The structure of **4** has been determined by X-ray analysis (Figure 2, Table 2 and 8).

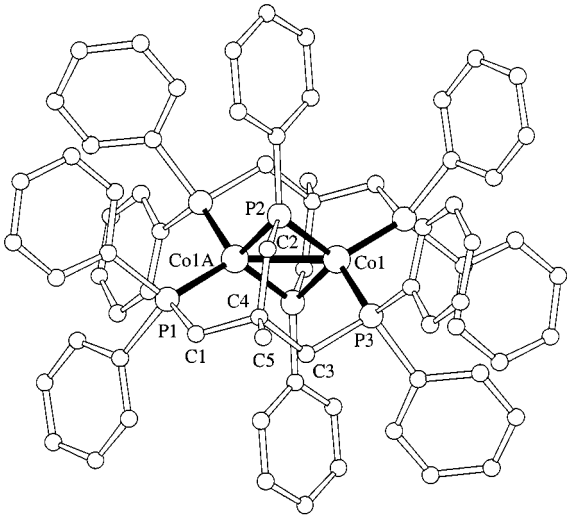

Figure 2. Structure of **4**, which has crystallographic inversion symmetry; atoms related to atom *i* by this symmetry are labelled as atom *i*A throughout

Table 2. Selected bond lengths [pm], bond angles [°], and torsion angles [°] in **4**

	4
Co1−P1A[a]	215.23(7)
Co1−P2	215.17(8)
Co1−P3	213.69(7)
Co1−P2A	216.07(7)
Co1−Co1A	233.41(6)
P1−C1	189.0(3)
P2−C2	184.7(3)
P3−C3	185.7(3)
$P-C_{Ph}$	183.3(3)−184.9(3)
$C_{CH_2}-C4$	155.0(4)−156.6(4)
P1A−Co1−P2	126.94(3)
P1A−Co1−P2A	95.11(3)
P1A−Co1−P3	113.24(3)
P2−Co1−P2A	114.46(2)
P2−Co1−P3	92.45(3)
P2A−Co1−P3	116.40(3)
P1A−Co1−Co1A	129.53(3)
P2A−Co1−Co1A	57.04(2)
P2−Co1−Co1A	57.42(2)
P3−Co1−Co1A	116.82(3)
Co1−P2−Co1A	65.54(2)
P2−Co1−P3−C3	56.1
Co1−P3−C3−C4	−65.7
P3−C3−C4−C2	5.2
C3−C4−C2−P2	50.4
C4−C2−P2−Co1	−42.5
C2−P2−Co1−P3	−13.3
P2−Co1A−P1−C1	−44.6
Co1A−P1−C1−C4	16.3
P1−C1−C4−C2	48.7
C1−C4−C2−P2	−75.8
C4−C2−P2−Co1A	32.3
C2−P2−Co1A−P1	23.7

[a] Atom labels refer to Figure 2. The molecular structure shows centrosymmetric symmetry. In Figure 2, the atom related to atom *i* by this symmetry is labelled as atom *i*A.

The formation of **4** from **1** may possibly be rationalized by considering that in THF solutions of **1** the *tripod* ligand is present in a bidentate binding mode with only two of its donor groups coordinated to the metal and the third one remaining as a dangling arm.[4] Since it has been shown that reductive dephenylation[9] of *tripod* ligands may occur in complexes as well as in the free ligand, it is tempting to assume that in the case of **1** the noncoordinated PPh_2 group is preferentially dephenylated. This assumption might explain the formation of the phosphido group of the ligand $[CH_3C(CH_2PPh_2)_2CH_2PPh]^-$ in **4**.

The molecules of **4** are centrosymmetric, containing a dicobalt unit at the centre. This unit is bridged by two CH_2PPh^- phosphido groups in a μ_2 manner. Each of these phosphido groups is part of one $[CH_3C(CH_2PPh_2)_2CH_2PPh]^-$ tripodal entity, with the two CH_2PPh_2 groups of each of these ligands coordinating to a Co centre (Figure 2). Each Co centre is thus coordinated by four P atoms in a coordination polyhedron that is best described as distorted tetrahedral, with the corresponding P−Co−P angles in the range 92.5−126.9° (Table 2). The binding mode of the $[CH_3C(CH_2PPh_2)_2CH_2PPh]^-$ ligand in **4** is similar to that observed for the $[CH_3C(CH_2PPh_2)_2CH_2S]^-$ ligand in $\{[CH_3C(CH_2PPh_2)_2CH_2S]_2Ni_2\}^{2+}$,[10] where the thiolate function acts as a μ_2 bridging group. In this dinickel compound, the coordination geometry about the Ni centres is idealized square planar, in contrast to the idealized tetrahedral surroundings of the Co centres in **4**. As a consequence, there is some strain in the chelate scaffolding of **4**. The six-membered chelate rings formed by the phosphido phosphorus, one phosphane donor, and the three-carbon chain at each of the two Co centres (Figure 2) have rather irregular twist conformations (torsion angles in Table 2). The most marked twists are seen along the sequences P2−Co1−P3−C3 (56.1°) and C3−C4−C2−P2 (50.4°). These torsion angles are of similar size and equal sign as characteristic for a twist conformation. The corresponding torsion angles P2−Co1A−P1−C1 (−44.6°) and C1−C4−C2−P2 (−75.8°) in the chelate cycle about Co1A are also similar in size and equal in sign as befits a twist conformation.

In terms of its bonding, **4** is an analogue of $(PMe_3)_4(\mu_2\text{-}PMe_2)_2Co_2$,[3c] in which the phosphane and phosphido groups act as isolated ligands as opposed to being covalently linked in **4**. The basic geometries of these two compounds are correspondingly similar. Both compounds show a planar $[Co_2(\mu_2\text{-}P_2)]$ cyclic arrangement with short transannular Co−Co distances of just 236 pm in the PMe_3 derivative and 233 pm in **4**. The short Co−Co distance in the

former has been interpreted in terms of the formation of a Co−Co double bond, in agreement with the diamagnetism of this compound as inferred from its NMR spectra. No NMR spectra of **4** could be recorded since, once crystallized, the compound proved to be insoluble in both apolar (toluene) and polar (CH_2Cl_2, DMA, THF) solvents. Although the diamagnetism of **4** has not been proved experimentally, the close similarity of the basic structural arrangements in $(PMe_3)_4(\mu_2\text{-}PMe_2)_2Co_2$ and **4** can be taken to indicate similar bonding.

A selective synthesis of **4** might be envisaged as being possible through the reaction of $[CH_3C(CH_2PPh_2)_2CH_2PPh]^-$ with Co salts under reductive conditions. For this purpose, the *tripod* ligand $CH_3C(CH_2PPh_2)_2CH_2PHPh$ (**6**), was synthesized from the easily accessible precursor $CH_3C(CH_2PPh_2)_2CH_2Cl$, **5** (Scheme 3).[10]

5 **6**

Scheme 3

Thus, a solution of **5** in DMSO was treated with a solution of PhPHK, prepared from KO*t*Bu and $PhPH_2$, in the same solvent, to furnish the *tripod* ligand **6**. After chromatographic workup, **6** was obtained as a viscous, colourless oil in 82% yield.

When a THF solution of **6** was treated with $CoCl_2$, a green solution was obtained, which, by analogy with the reaction of *tripod* with $CoCl_2$, could be expected to contain η^2-**6**·$CoCl_2$.

Addition of KC_8 to such a solution resulted in a brown slurry, from which minor amounts ($\leq$ 5%) of **4** could be isolated by crystallization. That **4** had indeed been formed was confirmed by the mass spectrum of the material produced, which was identical to those obtained from crystalline samples of **4** prepared starting from *tripod* (see above), as well as by comparison of the unit cell dimensions determined for crystals of the relevant samples.

The formation of **4** from *tripod*$CoCl_2$ under the strongly reducing conditions used to generate the dinitrogen compound **3** under an atmosphere of dinitrogen (Figure 1a) or a reactive species (Figure 1c) under argon is evidently a minor side reaction since all the other products described in this paper, as obtained from such strongly reducing solutions, are found to contain the intact $CH_3C(CH_2PPh_2)_3$ ligand showing no signs of dephenylation.

Reactivity of the Solutions Obtained from 1 or 2 by Reduction in THF under Argon

The THF solutions obtained by reducing *tripod*$CoCl_2$ (**1**), or *tripod*CoCl (**2**), with strong reducing agents such as KC_8 or Na/Hg under argon atmosphere all showed the same type of UV/Vis/NIR spectrum (Figure 1c). Irrespective of the coordination compound (**1** or **2**) or reductant (KC_8, Na/Hg) from which they are obtained (Table 1), these solutions are henceforth referred to as "solution **A**". Once formed, solution **A** does not react with N_2. The spectral signature remains unchanged when the argon atmosphere is replaced by N_2. Condidering their method of preparation, it is probable that these solutions contain [*tripod*Co] species with Co in a low oxidation state. With this in mind, it seemed appropriate to test their reactivity with regard to oxidative addition reactions. A series of substrates containing N−H, P−H, or Sn−H bonds as constituents potentially able to undergo oxidative addition was therefore tested.

N−H Functions

With $H_2N-NHPh$ as the substrate, initial oxidative addition might well be followed by a dehydrogenation reaction leading to compounds containing PhN_2H as the ligand.[11b] Since [*tripod*Co] compounds containing hydrazido ligands in a η^2 coordination mode are well-characterized species,[11] it was hoped that formation of any such products would be recognized by comparison with the authentic compounds. When solution **A** was treated with $H_2N-NHPh$, a colour change from red-brown to red was observed. Evaporation of the solvent left an oily residue, which solidified after repeated treatment with petroleum ether (boiling range 40−60 °C). FAB mass spectrometric analysis showed that this solid contained $[tripodCo(H)_3Cotripod]^+$ [*m*/*z* = 1369 (M^+)] and presumably also *tripod*Co(η^2-PhNNH) [*m*/*z* = 789 (M^+)]. The latter compound has previously been prepared from $[tripodCo(\eta^2\text{-}PhNNH_2)]^+$ by deprotonation[11b] All attempts to isolate it in a pure state from the above reaction were unsuccessful.

Besides N−H bond addition, the oxidative addition of hydrazine might also involve oxidative cleavage of the N−N bond. In order to obtain a model for the type of compound that might ensue from such an N−N bond scission, the diamido derivative $[tripodCo(\mu\text{-}NH_2)_2Cotripod](BPh_4)_2$ (**7**), was prepared from *tripod*$CoCl_2$, **1**, and $NaNH_2$ (Scheme 4).

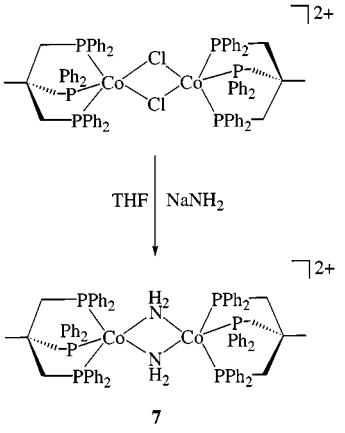

7

Scheme 4

The BPh_4^- salt of **7** was obtained as a microcrystalline brown powder and was completely characterized by all the appropriate analytical techniques (Table 6 and 7, see exp.

Section), including by single-crystal X-ray analysis (Figure 3).

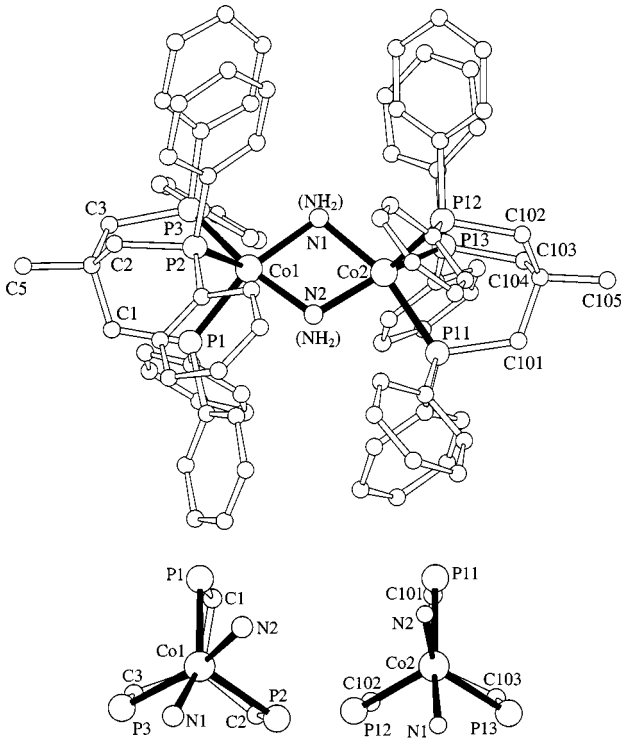

Figure 3. Structure of **7**: Bridging by the NH_2 groups is asymmetric (not shown); the individual positions of the bridging NH_2 groups could be refined using the split-atom technique; the bottom part of the figure shows the coordination polyhedra in a projection onto the relevant P_3 planes; the environment around Co1 (left-hand side) is idealized square pyramidal, while the coordination of Co2 is better described as idealized trigonal bipyramidal (right-hand side). Due to disorder problems, individual geometrical parameters are not accurate and hence are not explicitly given in this paper. Crystallographic data are nevertheless available (see exp. Section, X-ray Crystallographic Study).

Elucidation of the molecular structure of **7** is hampered by partial disorder of the bridging ligands. Its crystal structure is isotypical with that of [*tripod*Co(μ-OH)$_2$Co*tripod*](BPh$_4$)$_2$,[12] where the same type of disorder phenomena, with a minimum of two split positions for each OH group, has been found.[12] Although, in spite of this disorder, the constitution and overall geometry of **7** are clearly apparent, the individual distances and angles are subject to large errors. The Co−Co distance in **7** amounts to 308 pm, while that in its hydroxy analogue is 306 pm.[12] The Co−P distances range from 220 to 231 pm in **7**; in its OH analogue they lie in the range 223−229 pm.[12] The Co−N distances in **7** were determined as 197 pm and 189 pm, while the Co−O distances in the analogue measure 195 pm and 184 pm. It is clear from these figures that X-ray analysis cannot differentiate between the presence of μ-OH or μ-NH_2 bridges. The presence of μ-NH_2 bridges in **7** could, however, be proved by IR spectroscopy (CsI). The μ-OH groups in [*tripod*Co(μ-OH)$_2$Co*tripod*]$^{2+}$ give rise to an infrared absorption at 3260 cm^{-1}.[12] **7** shows no absorption in this region, but has absorptions at 3350 (m), 3313 (w), 3248 (m), 3197 (w), 3158 (w), and 3120 (w) cm^{-1} in the range characteristic for N−H vibrations. **7** crystallizes in the space group *P*1 with one molecule per unit cell such that no crystallographic symmetry restriction is imposed on it. The observed structure has no apparent symmetry higher than C_1 and hence four N−H vibrations are to be expected. The fact that six N−H vibrations are observed is in agreement with the observation that the individual NH_2 groups occupy different positions with respect to the [*tripod*Co Co*tripod*] entity, since the apparent disorder could be resolved by the split-atom technique. The coordination geometries about the Co centres are close to square pyramidal in one part of the molecule (Co1) and close to trigonal bipyramidal in the other part (Co2) (Figure 3, bottom). From these structural data, it appears that **7** may exist in different isomeric forms, a hypothesis that is supported by the fact that a total of six N−H bands are observed. The ESR data of the paramagnetic compound **7** [μ_{eff} (295 K) = 2.1 μ_B per molecule] are also in agreement with this hypothesis. Dichloromethane solutions of **7** show two signals at 298 K {g_1 = 2.11 [A_1 = 24 G]; g_2 = 2.09 [A_2 = 28 G]}. At least two different d^7 Co^{II} centres are therefore present in **7**. ESR spectra obtained in a CH_2Cl_2/THF glass at 100 K are not sufficiently resolved to determine the number of isomers present. An average *g* value of 2.11 and hyperfine coupling modulations corresponding to coupling constants of 34 G and 29 G are observed.

Having established the properties of **7**, the possibility of similar compounds having been formed in the reaction of solution **A** with $H_2N-NHPh$ can be ruled out. Reaction of solution **A** with NH_3 neither produced any species similar to **7**, nor could any secondary product resulting from this reaction be identified.

P−H Functions

In view of the well-documented capacity of [*tripod*Co] templates to generate[13] and bind ligands containing P−P bonds, $PhPH_2$ was tested as a substrate potentially able to undergo oxidative addition with the species present in solution **A**. While the initial product of this reaction could not be observed, the dehydrogenation product *tripod*Co(P_2Ph_2) (**8,** Scheme 5) was obtained in 44% yield. The reaction of solution **A** with $PhPH_2$ was accompanied by a gradual colour change from red-brown to red. Evaporation of the solvent left a red powder, from which analytically pure **8** was isolated by chromatography.

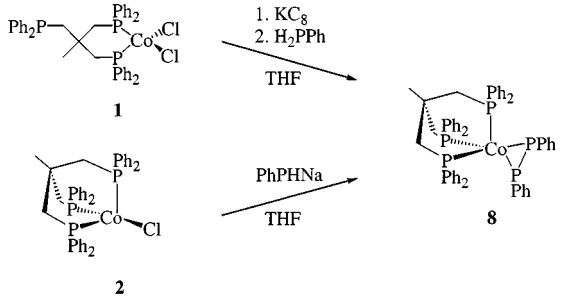

Scheme 5

Single crystals of **8** were obtained by layering a concentrated solution in acetone first with ethanol and then with

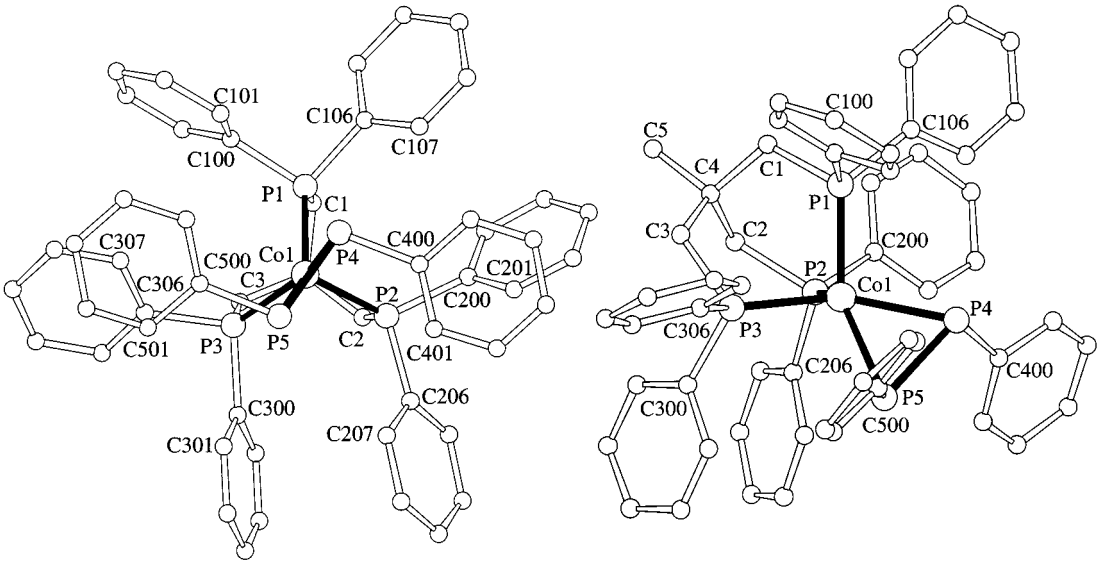

Figure 4. Structure of the diphosphene derivative **8**: Left-hand side: projection onto the plane formed by the three *tripod* phosphorus donor atoms; the torsion angles in Table 3 involving Hz_i refer to this projection; right-hand side: general view

petroleum ether (boiling range 40−60 °C). Its structure is shown in Figure 4 and the salient distances and angles are presented in Table 3. Crystallographic details are given in Table 8. The coordination geometry about cobalt may be viewed as idealized tetrahedral if the centre of the P−P bond is seen as occupying one corner of this idealized tetrahedron (Figure 4). In another view, an idealized square-pyramidal coordination geometry is apparent, with the two phosphorus centres of the diphosphene ligand, P4 and P5, and the two phosphorus donors of the *tripod* ligand, P1 and P3, forming the base and P2 the apex (Figure 4). Considering the distances between the phosphorus centres of the *tripod* ligand and the cobalt atom, this latter view appears to be more realistic since the apical bond Co1−P2 (225 pm) is significantly longer than the equatorial ones Co1−P1 (219 pm), Co1−P3 (219 pm) (see Table 3). The Co−P bonds involving the phosphorus centres of the diphosphene ligand are distinctly longer (234 pm, Table 3) than those to the *tripod* ligand. The distance P4−P5 (212.8 pm, Table 3) is characteristic of a side-on-coordinated P−P double bond. It is longer than the uncoordinated P−P double bond in free diphosphenes.[14−17] The diphosphene ligand in **8** shows a *trans* configuration (Figure 4). The bonds to the phenyl groups point slightly outwards, away from the Co atom. The torsion angle C400−P4−P5−C500 is 149°. This torsion is symmetrical with respect to the Co1−P4−P5 coordination plane, with the two torsion angles Co1−P4−P5−C500 (−103.3°) and Co1−P5−P4−C400 (−108.0°) being almost equal (Figure 4).

An independent synthesis of **8** was achieved by the reaction of *tripod*CoCl, **2**, with PhPHNa, which furnished the compound in 60% yield [a somewhat higher yield (70%) was obtained when *tripod*$CoCl_2$, **1**, was used as the starting compound]. The straightforward formation of **8** by reaction of PhPHNa with **1** or **2** is in contrast to the reaction of MesPHLi or IsPHLi (Mes = 2,4,6-trimethylphenyl, Is = 2,4,6-triisopropylphenyl) with these starting compounds.

Table 3. Selected bond lengths [pm], bond angles [°], and torsion angles [°] in **8**

	8
Co1−P1	219.31(9)
Co1−P2	225.01(9)
Co1−P3	219.37(8)
Co1−P4	233.60(9)
Co1−P5	234.07(9)
P4−P5	212.8(1)
P4−C400	184.1(3)
P5−C500	184.8(3)
P1−Co1−P2	90.61(3)
P1−Co1−P3	94.36(3)
P1−Co1−P4	100.86(3)
P1−Co1−P5	144.19(3)
P2−Co1−P3	90.95(3)
P2−Co1−P4	113.40(3)
P2−Co1−P5	121.45(3)
P3−Co1−P4	150.84(3)
P3−Co1−P5	100.08(3)
P4−Co1−P5	54.13(3)
Co1−P4−P5	63.05(3)
Co1−P4−C400	111.74(9)
P5−P4−C400	102.9(1)
Co1−P5−P4	62.82(3)
Co1−P5−C500	107.77(9)
P4−P5−C500	103.36(9)
Co1−P1−C1−C4	11.2
Co1−P2−C2−C4	18.2
Co1−P3−C3−C4	22.5
C400−P4−P5−C500	148.6
Co1−P4−P5−C500	−103.3
Co1−P5−P4−C400	−108.0
Hz1−P1−C100−C101[a]	15.0
Hz1−P1−C106−C107	51.7
Hz2−P2−C200−C201	32.6
Hz2−P2−C206−C207	32.7
Hz3−P3−C300−C301	15.4
Hz3−P3−C306−C307	57.4

[a] The torsion angles involving Hz at the bottom of the table are defined as follows: P−Hz designates a vector that is vertical with respect to the plane formed by the three *tripod* phosphorus donor atoms and points towards the observer when, in a projection onto this plane, the vector Co−C4 points away from the observer, such that C4 lies below this plane. [1c]

With these reactants, inseparable mixtures were obtained. Mass spectra gave no indication of the formation of products analogous to **8**. It thus appears that the bulky organic substituents (Mes, Is) impede the formation of the corresponding R_2P_2 ligands. Analysis of the product mixtures obtained from these bulky phosphanes is complicated by the fact that the compounds are paramagnetic, thus preventing the use of many analytical methods. This is a problem pertaining to many of the reactions described in this paper. The only reliable means of assessment is single-crystal X-ray analysis, which, however, requires suitable single crystals, which are not always easy to obtain.

Sn−H Functions

Next we analysed the reactivity of Sn−H functions in the given context. The reason for selecting stannanes as substrates was due to the fact that phosphane Co templates are known to form stable Co−Sn bonds.[3a] When solutions **A** were treated with Ph_3SnH, a slight colour change from red-brown to red was observed over a period of 12 hours. By chromatographic workup, the compound *tripod*$CoSnPh_3$ (**9**, Scheme 6), was isolated from the reaction mixture in yields of around 60%. **9** could also be obtained through the reaction of **2** with Ph_3SnLi. As an analogue of **9**, $(PMe_3)_3$-$CoSnPh_3$ [3a] has previously been prepared by Klein et al. by means of a salt metathesis reaction starting from $(PMe_3)_3CoCl$. The 16-electron d^8 compound **9** is paramagnetic, as expected for tetrahedral coordination. Its magnetic moment amounts to 3.2 μ_B, indicating the presence of two unpaired electrons. The UV/Vis/NIR spectrum of **9** (Table 7) exhibits features characteristic for compounds of the type *tripod*CoX[6] with one band at 950 nm (ε = 95) and a broad maximum at 1470 nm (ε = 170). In comparison with the spectrum of *tripod*CoCl {530 nm [ε = 120, sh], 826 nm [ε = 150], 1131 nm [ε = 430], 1224 nm [ε = 450]},[4] where the two long-wavelength bands are resolved into two individual maxima, the long-wavelength band of **9** must correspond to the envelope of two unresolved absorptions. The reaction of **2** with Ph_3SnLi could be monitored by UV/Vis/NIR spectroscopy. It was found that with the protocol described in the Experimental Section, the reaction is quantitative. Single crystals of **9** were obtained by layering THF solutions with petroleum ether (boiling range 40−60 °C).

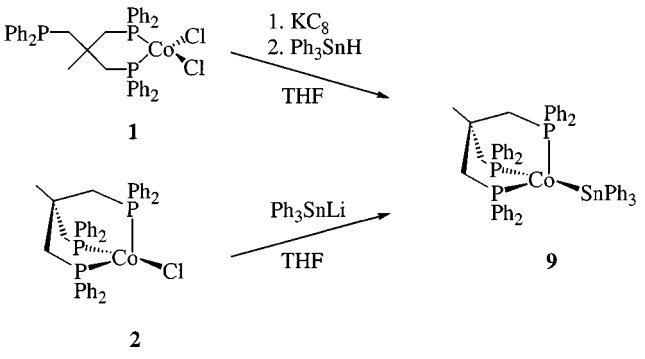

Scheme 6

X-ray analysis confirmed the idealized tetrahedral coordination of the Co centre in **9** (Figure 5). The mutual arrangement of the three phenyl groups of the $SnPh_3$ ligand and the six phenyl groups of the *tripod* ligand appears to impose steric problems. One of the phenyl groups of the *tripod* ligand (C100−C105 at P1) and one of the phenyl groups of the $SnPh_3$ unit (C400−C405) show disorder with respect to their rotational positions about their P−C_{ipso} and Sn−C_{ipso} axes, respectively. The positions shown for these groups in Figure 5 correspond to the orientation that is adopted by 70% of the molecules within the crystal.

The fact that this disorder is seen for both of these rings to approximately the same extent (relative occupancies of 70:30) indicates that the rotational motions of the phenyl groups are strongly coupled. It would appear that this steric interference is mirrored in the position of the tin centre. For an undisturbed molecule of the type *tripod*CoX, the ligand

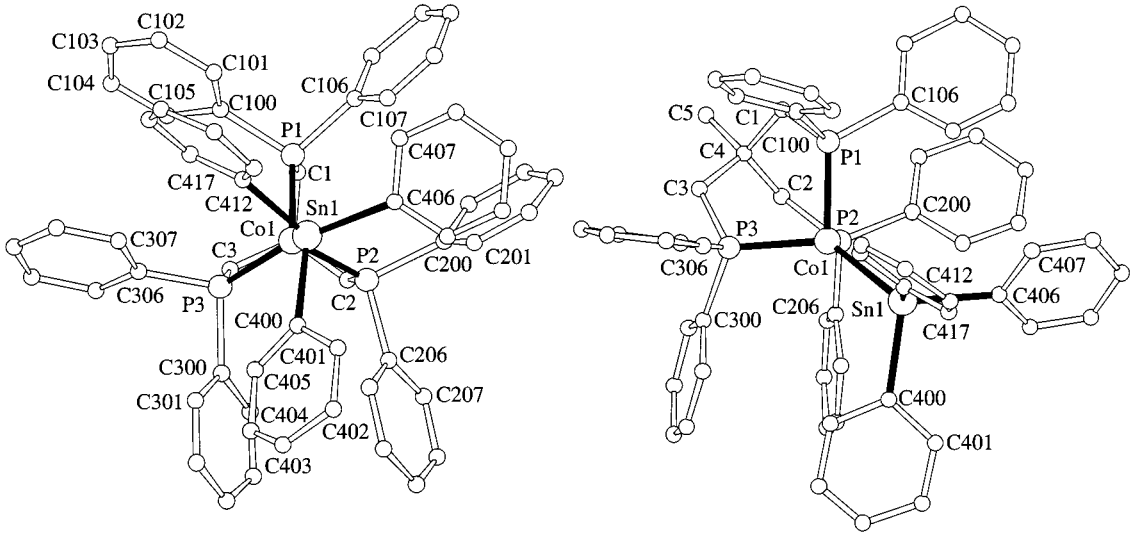

Figure 5. Structure of **9**: In the solid state the phenyl rings C100−C105 and C400−C405 are found to be disordered over two rotational positions in a 7:3 ratio; the major conformer is shown here; the left-hand figure corresponds to a projection of the structure onto the plane formed by the three *tripod* phosphorus donor atoms; the right-hand figure gives a general view of the compound

atom X would be expected to be located on the idealized trigonal axis of the P_3Co entity. This is indeed found for compounds such as *tripod*CoX (X = Cl,[4] Br,[6] NO[18]). In **9**, the tin centre shows a significant deviation from this coaxial position (Figure 5, left-hand side). The Co−P distances [219.6(3)−220.9(4) pm] are marginally shorter than those in *tripod*CoCl, **2** [224.2(3) pm][4] or $(PMe_3)_3CoSnPh_3$ [222(1) pm].[3a] The Co−Sn distance of 258.5(2) pm (Table 4) closely resembles that found in $(PMe_3)_3CoSnPh_3$ [259.0(2) pm].[3a]

In contrast to the reaction of Ph_3SnH with solution **A** [obtained by reduction of *tripod*$CoCl_2$ (**1**), with KC_8], which gives *tripod*$CoSnPh_3$, **9**, Bu_3SnH produces the dihydride compound *tripod*$Co(H)_2SnBu_3$, **10a** (Scheme 7).

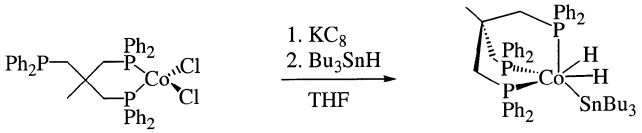

1 **10a**

Scheme 7

Table 4. Selected bond lengths [pm], bond angles [°], and torsion angles [°] in **9**, **10b**, and **11**

	9	**10b**[a]	**11**[b]
Co1−P1	220.9(4)	214.8(1)	220.9(1)
Co1−P2	219.6(3)	217.5(1)	218.7(1)
Co1−P3	220.6(3)	216.9(1)	217.7(1)
Co1−Sn1	258.5(2)	249.39(7)	256.14(7)
Co1−X	−	137(4)	171.0(4)
Co1−Y	−	135(4)	−
C6−O6	−	−	117.8(4)
Sn1−X	−	236	−
Sn1−Y	−	225	−
Sn1−C400	220(1)	219.5(4)	219.3(4)
Sn1−C406	220(1)	218.4(4)	217.7(4)
Sn1−C412	221(1)	217.8(5)	219.5(4)
P1−Co1−P2	91.0(1)	96.23(4)	97.55(4)
P1−Co1−P3	94.4(1)	93.06(5)	90.51(4)
P2−Co1−P3	92.4(1)	92.12(4)	90.66(4)
P1−Co1−Sn1	120.7(1)	139.75(4)	102.81(3)
P2−Co1−Sn1	118.07(9)	110.63(3)	95.77(3)
P3−Co1−Sn1	130.7(1)	114.50(4)	164.26(3)
P1−Co1−X	−	86(2)	133.3(1)
P2−Co1−X	−	178(2)	129.2(1)
P3−Co1−X	−	87(2)	89.1(1)
P1−Co1−Y	−	88(2)	−
P2−Co1−Y	−	88(2)	−
P3−Co1−Y	−	178(2)	−
X−Co1−Sn1	−	68(2)	75.7(1)
Y−Co1−Sn1	−	64(2)	−
X−Co1−Y	−	92(2)	−
C400−Sn1−Co1	114.1(2)	121.5(1)	111.4(1)
C406−Sn1−Co1	120.0(3)	121.2(1)	128.0(1)
C412−Sn1−Co1	119.0(3)	110.3(1)	113.8(1)
C400−Sn1−C406	101.5(4)	104.7(2)	102.3(2)
C400−Sn1−C412	100.2(4)	95.2(2)	97.3(1)
C406−Sn1−C412	98.6(4)	98.4(1)	99.3(1)
Co1−P1−C1−C4	7.4	22.2	23.0
Co1−P2−C2−C4	14.4	11.1	10.6
Co1−P3−C3−C4	14.2	16.2	18.6
Hz1−P1−C100−C101[c]	29.2	11.7	12.3
Hz1−P1−C106−C107	23.7	55.7	−14.9
Hz2−P2−C200−C201	15.0	22.3	47.9
Hz2−P2−C206−C207	26.2	36.9	29.1
Hz3−P3−C300−C301	26.9	32.2	24.3
Hz3−P3−C306−C307	29.8	26.2	35.5
Co1−Sn1−C400−C_{ortho}[d]	135.6	−97.5	−95.7
Co1−Sn1−C406−C_{ortho}[d]	90.7	−101.0	−142.9
Co1−Sn1−C412−C_{ortho}[d]	−170.7	178.9	−150.2

[a] **10b** with X = H1, Y = H2. − [b] **11** with X = C6−O6. − [c] The torsion angles involving Hz at the bottom of the table are defined as follows: P−Hz designates a vector that is vertical with respect to the plane formed by the three *tripod* phosphorus donor atoms and points towards the observer when, in a projection onto this plane, the vector Co−C4 points away from the observer, such that C4 lies below this plane [1c] (see Figures 5−7). − [d] C_{ortho} refers to the C atom that points towards the observer when viewed along the Sn−Co axis.

10a was obtained in the form of a yellow-brown crystalline material in about 50% yield after chromatographic separation. In accordance with its formal Co^{III} oxidation state, it is a diamagnetic compound. Its ^1H NMR spectrum shows well-resolved signals in the appropriate integral ratios for all the organic groups (Table 5). The signal due to the Co-bonded hydrogens is observed at $\delta = -13.4$ with a relative intensity corresponding to two protons. This signal shows satellites induced by ^{119}Sn coupling with a coupling constant of 170 Hz, which is clearly too small for covalent Sn−H bonding (*cf.* Ph_3SnH: $^1J_{^{119}SnH} = 1900$ Hz), but rather indicates a secondary interaction of the metal-bonded hydrogen atoms with the tin nucleus.

For compounds involving this type of agostic interaction, coupling constants in the range 150−330 Hz[19] have been found to be characteristic. $^2J_{PH}$ coupling is not resolved at 200 MHz, the only effect of ^{31}P decoupling being a marginal reduction in the line width. The presence of Co−H bonds in **10a** is also indicated by infrared absorptions at 1948 and 1909 cm^{-1} (Table 7), the intensities of which are similar to those of the C−H vibrations at around 3000 cm^{-1}. This high relative intensity rules out the possible interpretation that these two bands might originate from a harmonic or combination vibration. The energy of the vibrations corresponds to energies reported for Co−H vibrations in other hydride compounds.[20] The appearance of two $\tilde{\nu}$(Co−H) absorptions corresponds to the symmetric and antisymmetric vibrations. The $^{31}P\{^1H\}$ NMR spectrum of **10a** shows a broad resonance at $\delta = 46$ (line width 380 Hz). The appearance of this signal does not change significantly on cooling to 193 K, the only effect being a reduction of the line width (105 Hz). Observations of this nature have occasionally been made with [*tripod*Co^{III}] derivatives in the past.[2e] From this observation, it is evident that − over the temperature range studied − the relative orientation of the *tripod* ligand with respect to the coligands is dynamic. The ^{119}Sn NMR spectrum of **10a** shows one signal at $\delta = 17.8$ (Table 5), in the typical range for metal−bonded SnR_3 groups.[19b]

Cyclic voltammograms show − rather unexpectedly at first glance − that **10a** is reversibly oxidized at $E_{1/2} = -390$ mV. Since the formal oxidation state of the cobalt in compound **10a** is +III, oxidation of the metal would imply the formation of Co^{IV}, which is highly improbable given the nature of the ligands present. A possible explanation for this finding is the hypothesis that oxidation of **10a** leads to oxidative coupling of its hydride ligands to produce a η^2-coordinated dihydrogen ligand (Scheme 8).

Table 5. NMR spectroscopic data for compounds **10a**, **10b**, **11**

	^{1}H NMR	^{13}C{^{1}H} NMR	^{31}P{^{1}H} NMR	^{119}Sn NMR
10a[a]	−13.4 (s, $^1J_{^{119}SnH}$ = 170 Hz, 2 H, Co−*H*), 0.8 (m, 6 H, Bu-C*H*$_2$), 0.9 (m, 9 H, Bu-C*H*$_3$), 1.3−1.4 (m, 6 H, Bu-C*H*$_2$), 1.5−1.6 (m, 6 H, Bu-C*H*$_2$, 3 H *tripod*-C*H*$_3$), 2.3 (br. s, 6 H, C*H*$_2$P), 7.0−7.3 (m, 30 H, aromatic *H*)	14.2 (s, Bu-*C*H$_3$), 16.4 (s, Bu-*C*H$_2$), 28.8 (s, Bu-*C*H$_2$), 31.3 (s, Bu-*C*H$_2$), 36.4 (m, *C*H$_2$P), 37.9 (m, *tripod*-*C*H$_3$), 127.6−141.9 (aromatic *C*)	46.0 (m)	17.8 (m)
10b	−13.2 (s, $^1J_{^{119}SnH}$ = 220 Hz, 2 H, Co−*H*), 1.6 (s, 3 H *tripod*-C*H*$_3$), 2.3 (br. s, 6 H, C*H*$_2$P), 6.8−7.7 (m, 45 H, aromatic *H*)	36.1 (m, *C*H$_2$P), 37.8 (m, *tripod*-*C*H$_3$), 125.4−152.7 (aromatic *C*)	44.3 (m), 47.1 (m),[b] 43.8 (m)[b]	
11[a]	1.6 (s, 3 H *tripod*-C*H*$_3$), 2.4 (br. s, 6 H, C*H*$_2$P), 6.8−7.3 (m, 45 H, aromatic *H*)	36.4 (s, C_q), 37.1 (m, *C*H$_2$P), 38.1 (m, *tripod*-*C*H$_3$), 126.6−149.6 (aromatic *C*)	28.7 (br. s)	−31.4 (br. s)

[a] The data for **10a** were collected on a Bruker Avance DRX 300 instrument at 300.130 MHz (^{1}H), 121.495 MHz (^{31}P{^{1}H}), 75.468 MHz (^{13}C{^{1}H}); ^{13}C{^{1}H} NMR spectroscopic data for **11** were measured on a Bruker Avance DRX 500 spectrometer at 125.758 MHz; all the other data refer to measurements on a Bruker Avance DPX 200 instrument. − [b] T = 178 K.

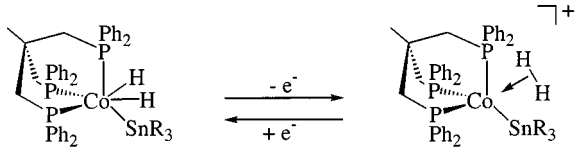

10a, b **B**

a: R = Bu
b: R = Ph

Scheme 8

In the 17-electron species **B** obtained after oxidation, cobalt is in its conventional +II oxidation state. Attempts to isolate **B** after oxidation of **10a** with ferrocenium salts have not yet been successful.

The fact that the 16-electron Co^{I} compound **9** and the 18-electron Co^{III} compound **10a** are both stable suggests that **9** should react with Lewis bases to form 18-electron Co^{I} compounds *tripod*CoSnPh$_3$L′.[21] This expectation is borne out by the reaction of **9** with carbon monoxide, which leads to the carbonyl derivative *tripod*Co(CO)SnPh$_3$ (**11**, Scheme 9).

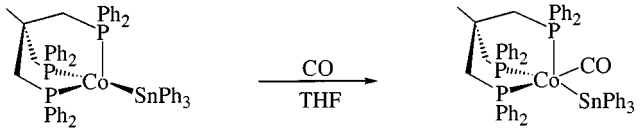

9 **11**

Scheme 9

Solutions of **9** change their colour from red to orange-yellow after a few minutes of exposure to carbon monoxide. From such a solution, **11** was isolated in 70% yield as a microcrystalline orange powder. Crystals were obtained by vapour diffusion of diethyl ether into a dichloromethane solution (Figure 6, Table 4 and 8)

The coordination of the cobalt centre in **11** is intermediate between trigonal bipyramidal and square pyramidal, as is often observed for compounds of the type *tripod*CoLL′. Angles and distances fall within their normal ranges (Table 4).

Analytical data (Table 6 and 7) and the NMR spectra (Table 5) of **11** are in full agreement with its constitution. The ^{119}Sn resonance is observed at δ = −31.4. Only one ^{31}P signal is observed, in agreement with the usual dynamic behaviour of five-coordinate compounds. No change in the appearance of the ^{31}P{^{1}H} NMR signal in the temperature range 293−193 K is observed. In the IR spectrum, the carbonyl group gives rise to a strong absorption at ν(CO) = 1853 cm^{-1} (Table 7). The cyclic voltammogram shows that the Co^{I} species **11** is reversibly oxidized at $E_{1/2}$ = −140 mV, indicating the relative stability of the cationic Co^{II} species [*tripod*Co(CO)SnPh$_3$]$^+$.

The carbonyl addition reaction of **9** is analogous to the reaction of (PMe$_3$)$_3$CoSnPh$_3$ with CO.[3a] In contrast to the (PMe$_3$)$_3$Co template, for which prolonged exposure of (PMe$_3$)$_3$Co(CO)SnPh$_3$ to CO leads to substitution of PMe$_3$ by CO, producing (PMe$_3$)$_2$Co(CO)$_2$SnPh$_3$, the *tripod* metal template of **11** remains unaffected. Solutions of **11** may be kept under CO for hours without any noticeable decomposition.

Comparing **9** with **10a**, the most plausible "oxidant" should be the dihydrogen. When a THF solution of **9** was stirred under 1 bar of H$_2$, the red colour of **9** was replaced by the yellow colour of **10b** within six hours (Scheme 10).

After chromatography, **10b** was isolated as a yellow microcrystalline powder. The ^{1}H NMR resonance of the hydride groups is observed at δ = −13.2, and ^{119}Sn satellites ($^1J_{^{119}SnH}$ = 220 Hz) indicate agostic HSn interactions.[19] In the IR spectrum, bands corresponding to the Co−H vibrations[20] are found at 1903 and 1888 cm^{-1} (Table 7). The intensities of these bands are again comparable to that of the strongest band in the ν̃(C−H) vibration region. The

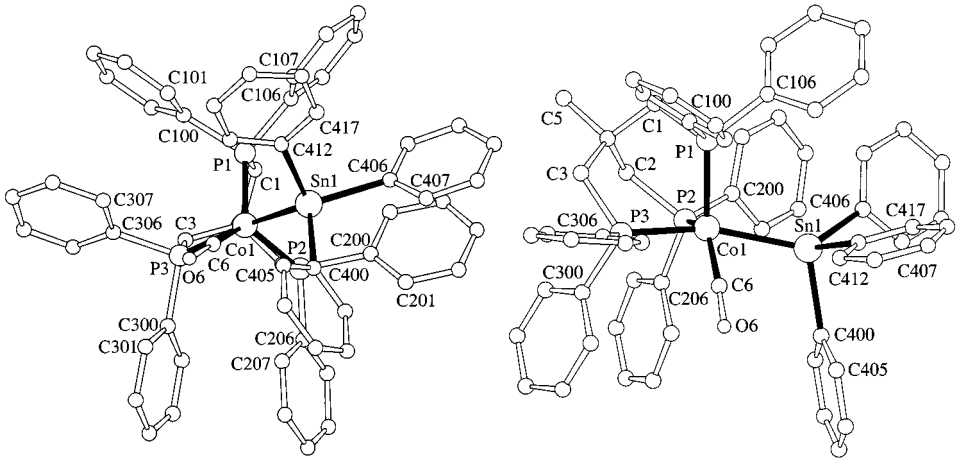

Figure 6. Structure of **11**: The left-hand side shows a projection onto the plane defined by the three *tripod* phosphorus donor atoms, the dummy vectors P_i-Hz_i in Table 4 refer to this view; the right-hand figure shows a general view of **11**

Table 6. Analytical data for compounds **7** to **11**

No.	Formula (M)	MS *m/z* (%) [Frag.]	$C_{calcd.}$ C_{found}	$H_{calcd.}$ H_{found}	$X_{calcd.}$ X_{found}	M.p. (°C)
7	$C_{130}H_{122}N_2P_6B_2Co_2\cdot 3CH_2Cl_2$	FAB: 1398 (1) [M^+], 1382 (6) [$M^+ - NH_4$],	69.68	5.63	1.22[a]	155
	2292.54	1322 (5) [$M^+ - Ph$], 698, (22) [M^{2+}], 683 (100) [*tripod*Co^+]	70.01	5.78	0.73[a]	(dec.)
8	$C_{53}H_{49}P_5Co$	EI: 899 (100) [M^+], 683 (87) [*tripod*Co^+]	70.75	5.49	17.21[b]	210
	899.77		70.59	5.49	17.04[b]	(dec.)
9[c]	$C_{59}H_{54}P_3CoSn$	–	68.56	5.27	8.99[b]	230
	1033.64		67.92	5.26	8.21[b]	
10a[c]	$C_{53}H_{68}P_3CoSn$	FAB: 931 (27) [$M^+ - Bu + O$]	65.25	7.03	9.52[b]	197
	975.69		64.89	7.01	8.19[b]	
10b[c]	$C_{59}H_{56}P_3CoSn$	FAB: 1034 (8) [$M^+ - 2$ H], 683 (27) [*tripod*Co^+]	–	–	–	171
	1035.64		–	–	–	(dec.)
11	$C_{60}H_{54}CoSnO$	FAB: 1062 (7) [M^+], 711 (8) [*tripod*Co(CO)$^+$], 683 (55)	67.88	5.13	8.75[b]	241
	1061.69	[*tripod*Co^+], 673 (100) [*tripod*O_3^+]	67.66	5.35	8.46[b]	(dec.)

[a] X = N. – [b] X = P. – [c] Compounds **9** and **10** are very air-sensitive. Due to this sensitivity, no microanalytical data could be determined for **10b** with the equipment available.

Table 7. Analytical data for compounds **7** to **11**

No.	CV Potential[a]	UV/Vis/NIR λ_{max} [nm] (ε) [$M^{-1}cm^{-1}$]	IR: $\tilde{\nu}$ [cm^{-1}]	μ_{eff} (μ_B) 295 K
7	E_p^C = −730mV (reverse scan: 40 mV); E_p^A = 970 mV (reverse scan: 270 mV)	344 (4120), 444 (725), 789 (420), 1175 (br, 140)[b]	N−H: 3350 (m), 3313 (w), 3248 (m), 3197 (w), 3158 (w), 3120 (w) [c]	2.1
8	$E_{1/2}$ = −65 mV (qrev. ox., ΔE = 100 mV), E_p^C = −610 mV (reverse scan: − 50 mV); E_p^A = 740 mV; ΔE_{Fc} = 190 mV	511 (sh, 1750), 681 (260), 1134 (br, 220)[d]	–	2.1
9	E_p^R = −30 mV (qrev. ox.,:ΔE = 125 mV); E_p^A = 170 mV, E_p^R = 355 mV; E_p^A = 1050 mV; E_p^C = −1270 mV; ΔE_{Fc} = 135 mV	485 (180), 593 (sh, 60), 949 (95), 1470 (br, 170)[d]	–	3.2
10a	$E_{1/2}$ = −390 mV (rev. ox.), ΔE = 145 mV; E_p^A = 860 mV, E_p^C = −1970 mV, ΔE_{Fc} = 140 mV	364 (sh, 870)[b]	Co−H: 1948 (m), 1909 (sh) [c]	–
	$E_{1/2}$ = −140 mV (rev. ox.), ΔE = 175 mV; E_p^A = 815 mV (reverse scan: 490 mV); ΔE_{Fc} = 135 mV	–	Co−H: 1903 (m), 1888 (m) [e]	–
11	$E_{1/2}$ = −140 mV (rev. ox.), ΔE = 105 mV; E_p^A = 1350 mV; ΔE_{Fc} = 135 mV	296 (19000), 344 (sh, 12000)[b]	CO: 1853 (vs) [c]	–

[a] All measurements were performed in CH_2Cl_2 solutions at scan speeds of 200 mVs^{-1}. – [b] Solvent: CH_2Cl_2. – [c] CsI. – [d] Solvent: THF. – [e] KBr.

$^{31}P\{^1H\}$ NMR spectrum of **10b** shows one signal at 298 K, which, in terms of its line width and shift, corresponds to that observed for **10a**. On cooling solutions of **10b** in CD_2Cl_2, the signal increases in intensity and starts to split into two components with an approximate ratio of 2:1 at 193 K. At 178 K, the lowest attainable temperature due to

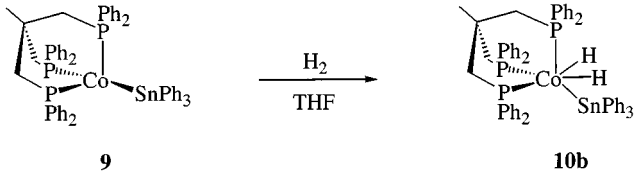

9 **10b**

Scheme 10

solubility problems, the individual absorptions are not yet separated and the signals are still broad (line width = 170 Hz).[2e] The signal with a relative intensity of one is seen at $\delta = 47$, that corresponding to a relative intensity of two at $\delta = 44$. Resolution of the individual resonances of the phosphorus nuclei of coordinated *tripod* ligands has occasionally been observed and has also been quantitatively analysed in terms of the rotation of the *tripod*Co template relative to the co-ligands.[5] The splitting of the $^{31}P\{^1H\}$ NMR signal of **10b** into two components with relative intensities of 2:1 indicates that the rigid conformation observed at low temperatures should have approximate C_S symmetry. Like **10a**, the Co^{III} compound **10b** was found to be reversibly oxidized. Oxidation occurs at $E_{1/2} = -140$ mV and, by the same arguments as discussed for **10a**, it is assumed that the oxidation process is not metal-centred but transforms the hydride ligands into a coordinated dihydrogen ligand leading to a compound of type **B** (Scheme 8).

The structure of **10b** has been elucidated by single-crystal X-ray analysis (Figure 7, Table 4 and 8).

Crystals of **10b** were obtained of exposing THF solutions of **10b** to a vapour phase of petroleum ether (boiling range 40−60 °C) for several days. The conformation adopted by **10b** in the solid state (Figure 7) is close to mirror symmetric with respect to the bonds radiating from the cobalt and tin centres (Figure 7, left-hand side). The rotational positions of the phenyl rings at P2 and P3 are also close to being mirror symmetric, within a range of about 30° (see torsion angles in Table 4). The rotational positions of the phenyl groups at the $SnPh_3$ ligand also conform to this idealized mirror symmetry, with the phenyl group C412−C417 lying in the mirror plane and the two remaining phenyl groups lying in positions mirror symmetric to each other [the torsion angles $Co-Sn-C_x-C_{ortho}$ refer to the *ortho* carbons C401, C407, and C417, as shown in Figure 7. This selection follows the convention of measuring the rotational positions of aryl groups with respect to the *ortho* carbon atom that is closest to the observer with respect to the projection shown in Figure 7 (left-hand side). With the selection of torsion angles thus made, a mirror symmetric arrangement of the phenyl groups of C400, C406 is indicated by torsion angles of equal size and equal sign, as is indeed found (−97.5° and −101.0°, Table 4)].

The approximate mirror symmetry exhibited by **10b** in the solid state must correspond to a globally optimal conformation since $^{31}P\{^1H\}$ NMR spectroscopy (see above) shows that the low-temperature conformation of **10b** is in fact mirror symmetric.

The positions of the hydride ligands have been inferred from electron density maps and refined by least-squares methods. The Co−H distances are around 136 pm, with an H−Co−H angle of around 90° (Table 4). The distances of these hydride ligands from the tin centre are around 230 pm (Table 4), making them definitely too long for a conventional Sn−H bond. Their interaction with the tin nucleus is nevertheless apparent from the Sn−H coupling constant of 220 Hz (Table 5). In spite of the fact that the cobalt centre is six-coordinate in **10b**, its coordination geometry is not octahedral (Figure 7, right-hand side). While all the Co-centred angles involving a phosphorus and a hydrogen ligand are close to 90° (or 180°, respectively; see Table 4), the angles involving the tin centre deviate from the ideal octahedral values by 20−30° throughout (Table 4). With **10b** being a Co^{III} derivative, the expected coordination polyhedron would be an octahedron. Considering the wealth of information available concerning the structures of six-coordinate Co^{III} compounds, **10b** represents a rare

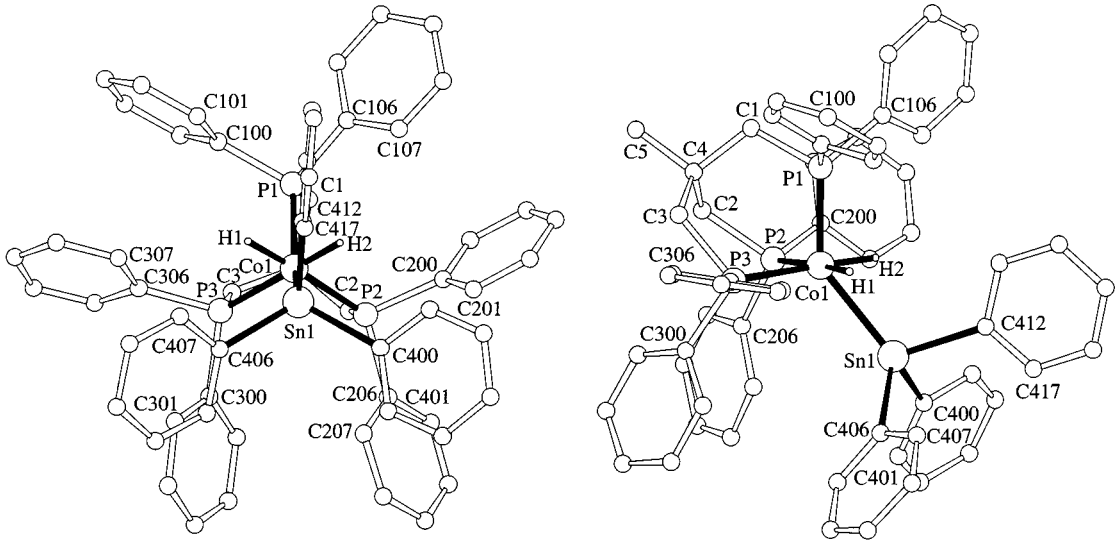

Figure 7. Structure of **10b**: The left-hand side diagram shows a projection of the structure onto the plane defined by the three *tripod* phosphorus donor atoms; the dummy vectors P_i-Hz_i in Table 4 refer to this view; the right-hand figure shows a general view of **10b**

Table 8. Crystal data for **4**, **7**, **8**, **9**, **10b**, and **11**

Compound	**4**	**7**	**8**	**9**	**10b**	**11**
Formula	$C_{70}H_{68}P_6Co_2\cdot 2.25\ CH_2Cl_2$	$C_{130}H_{122}P_6Co_2N_2B_2\cdot 1.5\ (CH_3)_2CO$	$C_{53}H_{49}P_5Co\cdot 0.75\ (CH_3)_2CO$	$C_{59}H_{54}P_3CoSn$	$C_{59}H_{56}P_3CoSn$	$C_{60}H_{54}P_3OCoSn\cdot 1.3\ CH_2Cl_2$
Molecular mass [g]	1404.01	2037.7	943.26	1033.64	1035.57	1171.97
Crystal size [mm]	0.2 × 0.25 × 0.25	0.3 × 0.2 × 0.2	0.2 × 0.2 × 0.15	0.2 × 0.2 × 0.1	0.15 × 0.2 × 0.2	0.05 × 0.2 × 0.3
Crystal system	triclinic	triclinic	monoclinic	monoclinic	orthorhombic	orthorhombic
Space group (No.)	$P\bar{1}$ (2)	$P1$ (1)	$P2_1/n$ (14)	$P2_1/n$ (14)	$Pna2_1$ (33)	$P2_12_12_1$ (19)
a [pm]	1110.80(2)	1389.1(3)	1347.5(3)	1402.7(3)	1919.0(4)	1359.8(3)
b [pm]	1149.30(2)	1561.7(3)	959.5(2)	1876.1(3)	1354.7(3)	1635.6(3)
c [pm]	1368.50(3)	1683.8(3)	3636.5(7)	1894.7(3)	1904.9(4)	2488.3(5)
α [°]	68.55(1)	114.77(1)	90	90	90	90
β [°]	86.73(1)	91.70(2)	96.98(3)	91.21(1)	90	90
γ [°]	81.14(1)	111.54(2)	90	90	90	90
V [10^6 pm^3]	1606.65(6)	3011(1)	4667(2)	4985(2)	4952(2)	5534(2)
Z	1	1	4	4	4	4
$d_{x.}$ [g cm^{-3}]	1.451	1.164	1.343	1.370	1.389	1.407
T [K]	200		200	200	200	200
No. of rflns. for cell param.	–	30	–	28	–	–
Scan range	4.9 ≤ 2Θ ≤ 56°	4.9 ≤ 2Θ ≤ 50°	3.1 ≤ 2Θ ≤ 52°	4.2 ≤ 2Θ ≤ 48°	3.7 ≤ 2Θ ≤ 56°	3.4 ≤ 2Θ ≤ 55°
Method	ω scan, Δω = 0.5°	ω scan, Δω = 0.6°	ω scan, Δω = 1.0°	ω scan, Δω = 0.6°	ω scan, Δω = 1.0°	ω scan, Δω = 1.0°
Scan speed	–	dω/dt = 10°min^{-1}	–	dω/dt = 10°min^{-1}	–	–
s frame^{-1}	20	–	5	–	2	3
No. rflns. measured	45008	10459	61896	8183	46221	49871
No. unique rflns.	6722	10459	9180	7829	11869	12711
No. rflns. observed	5786	7047	6488	4972	8885	10754
Observation criterion	$I \geq 2\sigma$	$I \geq 2\sigma$	$I \geq 2\sigma$	$I \geq 2\sigma$	$I \geq 2\sigma$	$I \geq 2\sigma$
No. param. refined	387	811	575	504	590	671
Resid. el. density [10^{-6} e pm^{-3}]	0.41	1.37	0.75	1.07	0.68	1.27
R_1/R_W [%] (refinement on F^2)	4.4/12.6	9.0/26.6	4.4/9.9	8.1/19.7	4.1/8.5	3.8/9.9

example of a significant deviation from the prototype octahedral coordination. Figure 7 (right-hand side) suggests that steric factors alone cannot be responsible for this observation. It thus appears that the agostic interactions between the cobalt-bonded hydrogens and the cobalt−tin bond might be the driving force for the observed distortion.

Conclusion

Solutions obtained by reduction of *tripod*$CoCl_2$ (**1**) or *tripod*CoCl (**2**) with electropositive metals in THF are highly reactive. Upon reaction with $PhPH_2$, they produce the diphosphene derivative *tripod*Co(η^2-PhP=PPh) (**8**). With R_3SnH they form *tripod*$CoSnR_3$ (**9**) or *tripod*$Co(H)_2SnR_3$ (**10**). The paramagnetic Co^I species *tripod*$CoSnPh_3$ undergoes oxidative addition of H_2 to produce *tripod*$Co(H)_2SnPh_3$ (**10b**). The Co^{III} compound **10b** is unique in so far as it has a very distorted octahedral geometry that allows for agostic H−Sn interactions and in that it undergoes reversible one-electron oxidation, which is assumed to be ligand-centred, producing the Co^{II} species [*tripod*Co(η^2-H_2)$SnPh_3$]$^+$.

Experimental Section

General Remarks: Unless otherwise noted, all manipulations were carried out under argon using standard Schlenk techniques. All solvents were dried by standard methods and distilled under argon or dinitrogen.[22] For ultrasonic activation of reaction mixtures, a "Bender & Hobein, Laboson 200" ultrasonic bath was used. The solvents CD_2Cl_2 and $CDCl_3$ used for NMR spectroscopic measurements were degassed by three successive "freeze-pump-thaw" cycles and dried with 4 Å molecular sieves. − NMR: Bruker Avance DPX 200 at 200.120 MHz (^{1}H), 50.323 MHz (^{13}C{^{1}H}), 81.015 MHz (^{31}P), and 74.631 MHz (^{119}Sn); T = 303 K unless stated otherwise; chemical shifts (δ) in ppm with respect to (residual protons in) CD_2Cl_2 (^{1}H: δ = 5.32; ^{13}C: δ = 53.80) and $CDCl_3$ (^{1}H: δ = 7.27; ^{13}C: δ = 77.00) as internal standards; ^{31}P chemical shifts (δ) in ppm with respect to 85% H_3PO_4 (^{31}P: δ = 0) as external standard. − IR: Bruker IFS-66; CsI or KBr discs or Nujol mulls. − EPR: Bruker ESP 300E (X-band, external standard diphenylpicrylhydrazyl). All measurements were made at 293 K and 100 K in a standard cavity ER 4102St. − Magnetic measurements: Faraday balance, Bruker B-E 15 C8 electromagnet, Bruker B-H 15 field controller, Sartorius M 25 D-S vacuum microbalance; calibration with $K_3[Fe(CN)_6]$. All measurements were carried out at 293 K. − UV/Vis/NIR: Perkin−Elmer Lambda 19. − Fast-atom bombardment (FAB) MS: Finnigan MAT 8230, xenon, matrix: 4-nitrobenzyl alcohol; electron impact (EI) MS: 70 eV. − Elemental analyses: Microanalytical Laboratory of the Organisch-Chemisches Institut, Universität Heidelberg. With the techniques used, problems arise with highly air- and temperature-sensitive compounds such as **9**, **10a**, and **10b** during the preparation of the test samples. The customary degree of accuracy is therefore not always attainable with these materials. The wet chemical analysis of phosphorus contents is occasionally disturbed by the presence of tin in the same sample. The corresponding analytical data will therefore also have higher margins of error. − Melting points: Gallenkamp MFB-595 010 apparatus; uncorrected values. − Cyclic voltammetry: Metrohm "Universal Meß- und Titriergefäß", Metrohm RDE 628 GC electrode, platinum electrode, SCE electrode, Princeton Applied Re-

search potentiostat model 273; samples 10^{-3} M in 0.1 M nBu_4NPF_6/CH_2Cl_2. Reactions described as reversible show a square-root dependence of current vs. scan speed in the range 50 to 1000 mVs^{-1}. All potentials are quoted relative to the saturated calomel electrode.

Materials: 1,1,1-Tris[(diphenylphosphanyl)methyl]ethane, *triphos*,[23] was prepared according to the literature procedure. All other materials were obtained from commercial sources and were used as received. Silica gel (Kieselgel z.A. 0.06−0.20 mm, J. T. Baker Chemicals B. V.) used for chromatography and kieselgur (Erg. B.6, Riedel de Haen AG) were degassed at 1 mbar for 24 h and saturated with argon.

General Procedure for the Synthesis of Solution A: A solution of **1**[4] (377 mg, 0.50 mmol) in THF (20 mL) was added to KC_8 (1.25 mmol), prepared by heating potassium (50 mg, 1.25 mmol) with graphite (120 mg, 10 mmol), and the suspension was sonicated until the colour changed to orange-brown. The reaction mixture was then filtered through kieselgur.

Synthesis of *tripod*Co(N_2)Co*tripod* (3): The following manipulations were carried out under a dry N_2 atmosphere:

Method a: A suspension of **2**[5] (359 mg, 0.50 mmol) in THF (20 mL) was added to KC_8 (1.50 mmol) and the mixture was sonicated until the colour turned to dark red. The supernatant reaction mixture was then removed from the insoluble material by means of a syringe. On layering this solution with petroleum ether (boiling range 40−60 °C), red crystals were obtained.

Method b: A solution of **1**[4] (377 mg, 0.50 mmol) in THF (20 mL) was added to activated Mg (2 g) (for activation: Mg filings were vigorously stirred in vacuo at 250 °C for 1 h) and the mixture was stirred until a dark-red colour developed. The supernatant reaction mixture was then removed from the unchanged Mg by means of a syringe. On layering this solution with petroleum ether (boiling range 40−60 °C), red crystals were obtained. − UV/Vis/NIR (THF): λ_{max} (ε) = 405 (8000), 718 (550), 1134 nm (4700 M^{-1} cm^{-1}). − Crystallographic data: see text.

Synthesis of [1,1-Bis(diphenylphosphanomethyl)-1-(phenylphosphanomethyl)]ethane (6): A solution of KO*t*Bu (689 mg, 6.14 mmol) and $PhPH_2$ (675 mg, 6.14 mmol) in DMSO (40 mL) was slowly added to a solution of 1-chloro-2-bis(diphenylphosphanylmethyl)propane (**5**)[10] (1.95 g, 4.10 mmol) in DMSO (30 mL). The reaction mixture was stirred for 4 h at 100 °C. The solvent was then removed in vacuo and the residue was purified by column chromatography on silica gel, eluting with petroleum ether (boiling range 40−60 °C)/diethyl ether, 9:1; R_f = 0.47. Yield: 1.84 g (3.35 mmol, 82%) as a colourless, viscous substance. − $C_{35}H_{35}P_3$ (548.58): calcd. C 76.63, H 6.43, P 16.94; found C 76.73, H 6.70, P 16.54. − ^{1}H NMR ($CDCl_3$): δ = 1.2 (br. s, 3 H, CH_3), 2.3 (br. s, 2 H, CH_2PHPh), 2.6 (br. s, 4 H, C$H_2$$PPh_2$), 4.0 (br. s, $^1J_{PH}$ = 204 Hz, 1 H, P*H*Ph), 6.9−7.9 (m, 25 H, arom. H). − ^{31}P NMR ($CDCl_3$): δ = −71.4 (d, $^1J_{PH}$ = 204 Hz, 1 P, PHPh), −26.8 (s, 2 P, PPh_2). − ^{13}C{^{1}H} NMR ($CDCl_3$): δ = 29.3 (m, CH_3), 37.3−38.3 (m, *C*H_2PHPh, Cq), 43.1 (m, *C*$H_2$$PPh_2$), 128.0−140.6 (arom. C). − MS (EI); *m*/*z* (%): 547 (17) [M^+ − H], 471 (100) [M^+ − Ph], 363 (19) [M^+ − PPh_2]. − IR (Nujol): $\tilde{\nu}$(P−H) = 2282 (vs) cm^{-1}.

Synthesis of [*tripod*Co(NH_2)$_2$Co*tripod*](BPh_4)$_2$ (7): To a solution of **1**[4] (754 mg, 1.00 mmol) in THF (40 mL) (blue solution) were added $NaBPh_4$ (342 mg, 1.00 mmol) (solution turned red) and $NaNH_2$ (78 mg, 2.00 mmol). After the colour of the mixture had turned brown, the solvent was removed in vacuo. The residue was redissolved in CH_2Cl_2, this solution was filtered through 5 cm kieselgur, and the solvent was removed to leave 682 mg (0.67 mmol, 67%) of a brown powder. Recrystallization from acetone/diethyl ether yielded orange crystals suitable for X-ray structure analysis (see exp. Section, X-ray Crystallographic Study). − EPR (CH_2Cl_2, 295 K): g_1 = 2.11 (A_1 = 24 G); g_2 = 2.09 (A_2 = 28 G). − EPR (THF/CH_2Cl_2, 100 K): g_{av} = 2.11 (A = 34, 29 G). − For additional analytical data, see Table 6 and 7.

Synthesis of *tripod*Co(P_2Ph_2) (8). − Method a: At −60 °C, a solution of **1**[4] (566 mg, 0.75 mmol) in THF (30 mL) was added to a solution of PhPHLi [24b] (1.65 mmol), prepared by adding *n*BuLi (0.66 mL, 2.5 M in hexane) to a solution of $PhPH_2$ (182 mg, 0.18 mL, 1.65 mmol) in THF (20 mL). The colour changed from blue to red and the mixture was stirred for 30 min. at room temperature. The solvent was then removed in vacuo, and the residue was suspended in petroleum ether (boiling range 40−60 °C) and flash chromatographed on silica gel. After elution with 200 mL of petroleum ether (boiling range 40−60 °C), the product was eluted with diethyl ether as a red band, removal of the solvent from which gave 485 mg (0.54 mmol, 72%) of a microcrystalline powder. Red crystals, suitable for X-ray structure analysis, were obtained by layering a saturated acetone solution with ethanol and petroleum ether (boiling range 40−60 °C).

Method b: To solution **A**, prepared from **1**[4] (0.50 mmol) and KC_8 (1.25 mmol) (see above), was added $PhPH_2$ (170 mg, 0.17 mL, 1.54 mmol). After stirring for 2 h, the colour had changed to red and the solvent was removed in vacuo. The residue was taken up in petroleum ether (boiling range 40−60 °C). Chromatographic workup as described above gave 198 mg (0.22 mmol, 44%) of **8**.

Method c: A modification of Method a, starting from **1**[4] (566 mg, 0.75 mmol) and PhPHNa [24a] (1.65 mmol) [prepared by adding Na (38 mg, 1.65 mmol) to a solution of $PhPH_2$ (182 mg, 0.18 mL, 1.65 mmol) in THF (20 mL) and sonicating until the Na had dissolved] gave 472 mg (0.53 mmol, 70%) of compound **8**.

Method d: In a further modification of Method a, **8** was prepared starting from **2**[5] (359 mg, 0.50 mmol) suspended in THF (25 mL) and a solution of PhPHLi [24b] or PhPHNa[24a] (1.10 mmol) in THF (20 mL). Yield: 270 mg (0.30 mmol, 60%). − For analytical data, see Table 6 and 7.

Synthesis of *tripod*CoSnPh_3 (9). − Method a: A suspension of **2**[5] (359 mg, 0.50 mmol) in THF (15 mL) was added to a THF solution of Ph_3SnLi[25] (0.90 mmol), prepared by adding *n*BuLi (0.36 mL, 2.5 M in toluene) to a solution of Ph_3SnH (315 mg, 0.90 mmol) in THF (15 mL). The initially brown suspension turned red and the reaction mixture was stirred overnight. After removal of the solvent, the residue was suspended in petroleum ether (boiling range 40−60 °C) and flash chromatographed on silica gel. After elution with 200 mL of petroleum ether (boiling range 40−60 °C), the product was eluted with diethyl ether as a red band, removal of the solvent from which gave 340 mg (0.33 mmol, 66%) of a red microcrystalline powder. Red crystals, suitable for X-ray structural analysis, were obtained by layering a saturated THF solution with petroleum ether (boiling range 40−60 °C).

Method b: Compound **9** was prepared by adding Ph_3SnH (895 mg, 2.55 mmol) to solution **A**, prepared from **1**[4] (0.85 mmol) and KC_8 (2.13 mmol) (see above), and stirring overnight. Chromatographic workup (as described above) yielded 540 mg (0.52 mmol, 61%) of **9**. − For analytical data, see Table 6 and 7.

Synthesis of *tripod*Co($H)_2SnBu_3$ (10a): To solution **A**, prepared from **1**[4] (0.85 mmol) and KC_8 (2.13 mmol) (see above), was added

Bu_3SnH (745 mg, 0.68 mL, 2.56 mmol). After stirring overnight, the solvent was removed in vacuo. The residue was suspended in petroleum ether (boiling range 40−60 °C). Chromatographic workup (as described for compound **9**) gave 410 mg (0.42 mmol, 50%) of a yellow-brown microcrystalline solid. Recrystallization from acetone at −20 °C afforded 210 mg (0.22 mmol, 25%) as yellow crystals. − For analytical data, see Table 6 and 7.

Synthesis of *tripod*Co(H)$_2$SnPh$_3$ (10b): A solution of **9** (620 mg, 0.60 mmol) in THF (30 mL) was saturated with H_2 at 1 bar and stirred for 6 h. The red colour of the reaction mixture turned yellow. After removal of the solvent, the residue was suspended in petroleum ether (boiling range 40−60 °C). Chromatographic workup (as described for compound **9**) gave upon removal of the solvent 420 mg (0.41 mmol, 68%) of a yellow microcrystalline powder. A concentrated THF solution was distributed between several test tubes (Ø = 1 cm), which were placed in a Schlenk tube (250 mL). Petroleum ether (boiling range 40−60 °C) was introduced into the Schlenk tube, vapour diffusion of which into the THF solutions yielded yellow single crystals suitable for X-ray structure analysis. − For analytical data, see Table 6 and 7.

Synthesis of *tripod*Co(CO)SnPh$_3$ (11): CO was bubbled through a solution of **9** (620 mg, 0.60 mmol) in THF (30 mL) for 10 min. The red colour of the solution turned orange. The solvent was then removed in vacuo, the residue was suspended in petroleum ether (boiling range 40−60 °C), and chromatographed on kieselgur. After elution with 200 mL of petroleum ether (boiling range 40−60 °C), the orange product was eluted with toluene. Removal of the solvent in vacuo from the appropriate fraction gave 445 mg (0.42 mmol, 70%) of **11** as an orange microcrystalline solid. A concentrated dichloromethane solution was distributed between several test tubes (Ø = 1 cm), which were placed in a Schlenk tube (250 mL). Diethyl ether was introduced into the Schlenk tube, vapour diffusion of which into the CH_2Cl_2 solutions yielded orange single crystals suitable for X-ray structure analysis. − For analytical data, see Table 6 and 7.

X-ray Crystallographic Study: Measurements were made on a Siemens P4 four-circle diffractometer (**7**, **9**) or on a Nonius-Kappa CCD diffractometer (**4**, **8**, **10b**, **11**) using graphite-monochromated Mo-K_α radiation throughout. For the measurements on the Siemens P4 four-circle diffractometer, the intensities of three check reflections (measured every 100 reflections) remained constant throughout the data collection, thus indicating crystal and electronic stability. The data collected on the Siemens P4 diffractometer were corrected in the usual manner, including by an experimental absorption correction. The data collected on the Nonius Kappa CCD device were processed using the standard Nonius software.[26] All calculations were performed using the SHELXT-PLUS software package. Structures were solved by direct methods with the SHELXS-97 program and refined with the SHELXL-97 program.[27,28] Graphical handling of the structural data during solution and refinement was performed with XPMA.[29] Structural representations were generated using Winray 32.[30] Atomic coordinates and anisotropic thermal parameters of nonhydrogen atoms were refined by full-matrix least-squares calculations. The data relating to the structure determinations are compiled in Table 8. Compound **7**: The nitrogens of the amido groups are disordered over two positions with s.o.f.s of 0.75 and 0.25. The acetone solvent molecules were found to be distributed over four sites with s.o.f.s of 0.5, 0.4, 0.35, and 0.25. The disordered atoms were refined isotropically. Due to these disorder problems, the refinement converged only to $R_1 = 9.0\%$ and $R_2 = 26.6\%$, hence discussion of the bond lengths and angles is omitted. Compound **9**: One phenyl ring (C100−C105) was found to be disordered over two orthogonal orientations with s.o.f.s of 0.7 and 0.3. These atoms were refined isotropically. One phenyl ring of the $SnPh_3$ ligand (C400−C405) was found to be disordered over two rotational positions with s.o.f.s of 0.6 and 0.4. The angle between the orientations is 40°. Compound **10b**: The crystal of **10b** examined was found to be a racemic twin, the Flack *x* parameter being 0.267. The metal-bonded hydrogens H1 and H2 were located in the difference map and refined isotropically.

Crystallographic data (excluding structure factors) for the structures reported in this paper have been deposited with the Cambridge Crystallographic Data Centre as supplementary publication nos. CCDC-143127 (**4**), CCDC-143131 (**7**), CCDC-143130 (**8**), CCDC-143129 (**9**), CCDC-143126 (**10b**), and CCDC-143128 (**11**). Copies of the data can be obtained free of charge on application to the CCDC, 12 Union Road, Cambridge CB2 1EZ, U.K. [Fax: (internat.) +44 (0)1223/336033; E-mail: deposit@ccdc.cam.ac.uk].

Acknowledgments

We are grateful to the German Science Foundation (DFG), SFB 247, the VW Foundation (Stiftung Volkswagenwerk), and the Fonds der Chemischen Industrie for financial support. The technical support of T. Jannack (mass spectrometry), D. Günauer (cyclic voltammetry), and the Microanalytical Laboratory of the Institute of Organic Chemistry is gratefully acknowledged.

[1] For cobalt(II), see for instance: [1a]L. Sacconi, F. Mani, *Trans. Met. Chem*. **1982**, *8*, 179−252. − [1b]V. Sernau, G. Huttner, M. Fritz, B. Janssen, M. Büchner, C. Emmerich, O. Walter, L. Zsolnai, D. Günauer, T. Seitz, *Z. Naturforsch*. **1995**, *50b*, 1638−1652. − [1c]S. Beyreuther, J. Hunger, G. Huttner, S. Mann, L. Zsolnai, *Chem. Ber*. **1996**, *129*, 745−757.

[2] For cobalt(III), see for instance: [2a]R. B. King, L. W. Houk, K. H. Panell, *Inorg. Chem*. **1969**, *8*, 1042−1048. − [2b]C. Bianchini, D. Masi, C. Mealli, A. Meli, G. Martini, F. Laschi, P. Zanello, *Inorg. Chem.* **1987**, *26*, 3683−3693. − [2c]S. Vogel, G. Huttner, L. Zsolnai, *Z. Naturforsch*. **1993**, *48b*, 641−652. − [2d]C. A. Ghilardi, F. Laschi, S. Midollini, A. Orlandini, G. Scapacci, P. Zanello, *J. Chem. Soc., Dalton Trans.* **1995**, 531−540. − [2e]K. Heinze, G. Huttner, L. Zsolnai, A. Jacobi, P. Schober, *Chem. Eur. J.* **1997**, *3*, 732−743.

[3] See for instance: [3a]H.-F. Klein, K. Ellrich, D. Neugebauer, O. Orama, K. Krüger, *Z. Naturforsch.* **1983**, *38b*, 303−310. − [3b]D. A. Buckingham, C. R. Clark, *Comprehensive Coordination Chemistry*, Pergamon Press, **1987**, *Vol. 4*, 635−900. − [3c]H.-F. Klein, M. Gaß, U. Zucha, B. Eisenmann, *Z. Naturforsch*. **1988**, *43b*, 927−932. − [3d]H.-F. Klein, X. Li, H. Sun, A. Brand, M. Lemke, U. Flörke, H.-J. Haupt, *Inorg. Chim. Acta* **2000**, *298 (1)*, 70−75.

[4] K. Heinze, G. Huttner, L. Zsolnai, P. Schober, *Inorg. Chem*. **1997**, *36*, 5457−5469.

[5] R. Rupp, A. Frick, G. Huttner, P. Rutsch, U. Winterhalter, A. Barth, P. Kircher, L. Zsolnai, *Eur. J. Inorg. Chem.* **2000**, *3*, 523−536.

[6] L. Sacconi, S. Midollini, *J. Chem. Soc., Dalton Trans.* **1972**, 1213−1216.

[7] F. Cecconi, C. A. Ghilardi, S. Midollini, S. Moneti, A. Orlandini, M. Bacci, *J. Chem. Soc., Chem. Commun*. **1985**, 731−733.

[8] F. Cecconi, C. A. Ghilardi, S. Midollini, S. Moneti, A. Orlandini, *J. Organomet. Chem*. **1987**, *323*, C5−C9.

[9] [9a]O. Walter, T. Klein, G. Huttner, L. Zsolnai, *J. Organomet. Chem*. **1993**, *458*, 63−81. − [9b]M. Büchner, G. Huttner, U. Winterhalter, A. Frick, *Chem. Ber./Recueil* **1997**, *130*, 1379−1392. − [9c]O. Walter, M. Büchner, G. Huttner, *J. Organomet. Chem*. **1997**, *529*, 103−106.

[10] G. Rheinhard, R. Soltek, G. Huttner, A. Barth, O. Walter, L. Zsolnai, *Chem. Ber*. **1996**, *129*, 97−108.

[11] [11a] S. Vogel, A. Barth, G. Huttner, Th. Klein, L. Zsolnai, R. Kremer, *Angew. Chem*. **1991**, *103*, 325−327; *Angew. Chem. Int. Ed. Engl*. **1991**, *30*, 303−304. − [11b] V. Körner, G. Huttner, S.

Vogel, A. Barth, L. Zsolnai, *Chem. Ber./Recueil* **1997**, *130*, 489−492.
[12] C. Mealli, S. Midollini, L. Sacconi, *Inorg. Chem*. **1975**, *14*, 2513−2521.
[13] See for instance: [13a] M. Di Vaira, C. A. Ghilardi, S. Midollini, L. Sacconi, *J. Am. Chem. Soc*. **1978**, *100*, 2550−2551. – [13b] M. Di Vaira, L. Sacconi, *Angew. Chem*. **1982**, *94*, 338−351, *Angew. Chem. Int. Ed. Engl*. **1982**, *21*, 330. – [13c] M. Di Vaira, L. Sacconi, P. Stoppioni, *J. Organomet. Chem*. **1983**, *250*, 183−195. – [13d] A. Barth, G. Huttner, M. Fritz, L. Zsolnai, *Angew. Chem*. **1990**, *102*, 956−958, *Angew. Chem. Int. Ed. Engl.* **1990**, *29*, 929.
[14] M. Yoshifuji, I. Shima, N. Inamoto, K. Hirotsu, T. Higuchi, *J. Am. Chem. Soc*. **1981**, *103*, 4587−4589. For more recent examples, see refs.[15,16]
[15] L. Weber, *Chem. Rev.* **1992**, *92*, 1839−1906.
[16] CSD: F. H. Allen, J. E. Davis, J. J. Galloy, O. Johnson, O. Kennard, C. F. Macrae, E. M. Mitchell, G. F. Mitchell, J. M. Smith, D. Watson, *J. Chem. Inf. Comput. Sci*. **1991**, *31*, 187−204.
[17] For an early example concerning the bond lengths of η^2-side-on-coordinated *versus* free P−P double bonds, see ref.[15] – [17a] J. Borm, L. Zsolnai, G. Huttner, *Angew. Chem.* **1983**, *95*, 1018; *Angew. Chem. Int. Ed. Engl.* **1983**, *22*, 977.
[18] [18a] P. Dapporto, S. Midollini, A. Orlandini, L. Sacconi, *Inorg. Chem*. **1976**, *15*, 2768−2774. – [18b] S. Vogel, G. Huttner, L. Zsolnai, C. Emmerich, *Z. Naturforsch*. **1993**, *48b*, 353−363.
[19] [19a] U. Schubert, S. Gilbert, S. Mock, *Chem. Ber*. **1992**, *125*, 835−837. – [19b] S. Gilbert, M. Knorr, S. Mock, U. Schubert, *J. Organomet. Chem*. **1994**, *480*, 241−254.
[20] A. Sacco, R. Ugo, *J. Chem. Soc.* **1964**, *3*, 3274−3277.
[21] D. L. DuBois, D. W. Meek, *Inorg. Chem*. **1976**, *15*, 3076−3083.
[22] Organikum, Deutscher Verlag der Wissenschaften, Berlin, **1990**.
[23] A. Muth, Diplomarbeit, University of Heidelberg, **1989**.
[24] [24a] R. Batchelor, T. Birchall, *J. Am. Chem. Soc*. **1982**, *104*, 674−679. – [24b] Z. Hou, T. L. Breen, D. W. Stephan, *Organometallics* **1993**, *12*, 3158−3167.
[25] A. G. Davies, *Organotin Chemistry*, VCH, Weinheim, **1997**, *Chapter 17*, 253.
[26] DENZO−SMN, Data processing software, Nonius **1998**; http://www.nonius.com
[27] [27a] G. M. Sheldrick, *SHELXS-97, Program for Crystal Structure Solution*, University of Göttingen, **1997**; http://shelx.uni-ac.gwdg.de/shelx/index.html – [27b] G. M. Sheldrick, *SHELXL-97, Program for Crystal Structure Refinement*, University of Göttingen, **1997**; http://shelx.uni-ac.gwdg.de/shelx/index.html
[28] *International Tables for X-ray Crystallography*, Vol. 4, Kynoch Press, Birmingham, U.K., **1974**.
[29] L. Zsolnai, G. Huttner, *XPMA*; http://www.rzuser.uni-heidelberg.de/~v54/xpm.html, Universität Heidelberg, **1994**.
[30] R. Soltek, *Winray 32*; http://www.rzuser.uni-heidelberg.de/~v54/xpm.html, Universität Heidelberg, **2000**.

Received April 17, 2000
[I00148]